Influence of matrix toughness and ductility on the compression-after-impact behavior of woven-ply thermoplastic- and thermosetting-composites: A comparative study

B. Vieille [a,*], V.M. Casado [b], C. Bouvet [b]

[a] INSA Rouen – Groupe de Physique des Matériaux, UMR 6634 CNRS, 76801 St Etienne du Rouvray, France
[b] Univ. de Toulouse, INSA, UPS, Mines Albi, ISAE, ICA, 10 av. E. Belin, 31055 Toulouse Cedex 4, France

ARTICLE INFO

Keywords:
Polymer–matrix composites
Woven fabrics
Impact behavior
Residual properties

ABSTRACT

This study was aimed at comparing the residual compressive strength and behavior of TS-based (epoxy) and TP-based (PPS or PEEK) laminates initially subjected to low velocity impacts. Provided that the impact energy is not too low, the permanent indentation is instrumental in initiating laminates local buckling under compressive loadings. CAI tests revealed that matrix toughness is not the primary parameter ruling the damage tolerance of the studied materials. However, matrix ductility seems to slow down the propagation of transverse cracks during compression thanks to plastic micro-buckling which preferentially takes place at the crimps in woven-ply laminates. It could therefore justify why the matrix toughness of TP-based laminates does not result in significantly higher CAI residual strengths. Finally, the compressive failure mechanisms of impacted laminates are discussed depending on matrix nature, with a particular attention paid to the damage scenario (buckling and propagation of 0° fibers failure).

1. Introduction

Low velocity impact is one of the most detrimental solicitations for laminates because it drastically reduces the residual mechanical properties of the structure [1–3]. It is well established that polymer matrix composite laminates are prone to delamination when impacted, resulting in low damage tolerance, which is of great concern for load carrying applications. To discuss the damage tolerance of polymer matrix composites it is initially helpful to consider the nature of constitutive materials and the reinforcement type [4]. Thus, high-performance thermoplastic (denoted TP) resins (e.g. polyetheretherketone – PEEK – and polyphenylenesulfide – PPS) are increasingly considered in composite structures mainly for damage tolerance reasons. Semi-crystalline TPs resins offer a number of advantages over conventional thermosetting (denoted TS) resins (such as epoxies): a high degree of chemical resistance, excellent damage and impact resistances, and they may be used over a wide range of temperatures.

1.1. About damage tolerance of TS- and TP-based laminates

Very few authors have compared the impact behavior of TS- and TP-based composite structures, and their effects on residual strength [5–10], as well as the damage tolerance of UD-ply and woven-ply laminates [10–12]. From a general standpoint, it appears from literature that TP-based composites display a better resistance to the impact damage than epoxy-based composites. The brief literature review, herein, is not aimed at giving a general overview of the impact behavior of TS-based laminates for which a great number of references are available in the literature [1,13–15]. In the early 90s, the impact performance and damage tolerance of TP-based composites had been studied in order to understand why such materials were often more damage tolerant than TS-based composite materials [16–17]. To this aim, a few authors have investigated the influence of matrix type and morphology on the ability of TP-based composites to withstand penetration [18–19], absorb energy, and sustain damage at different temperature levels. Most of the studies about the impact performance, and damage tolerance of TP-based composites deal with PEEK-based composites [8,9,20–24]. However, only very few references report the impact behavior of PPS-based laminates [7,20,25–28]. The impact energy adversely affects the impact performance of the laminates, whereas the effect of impact velocity is found to be insignificant. Among the properties governing the impact behavior of laminated composites, the mode I and mode II critical energy release rates G_{IC} and G_{IIC} (see Table 1) are of the utmost importance [29–32]. In addition, higher Compression After Impact (CAI) strengths are generally observed in C/PEEK compared to C/Epoxy (see Fig. 1a), and the reason has already been explained [8,28].

* Corresponding author.
E-mail address: benoit.vieille@insa-rouen.fr (B. Vieille).

Table 1
Interlaminar fracture toughness of tested materials [43].

	C/PEEK	C/PPS	C/Epoxy (914)
G_{Ic} (kJ/m^2) neat resin	4	0.5–0.9	0.1
$G_{Ic,initiation}$ (kJ/m^2) carbon fiber woven-ply polymer	1.1–2.1	0.85–1	0.35–0.5
$G_{IIc,initiation}$ (kJ/m^2) carbon fiber woven-ply polymer	2–4.9	1.8	1.5

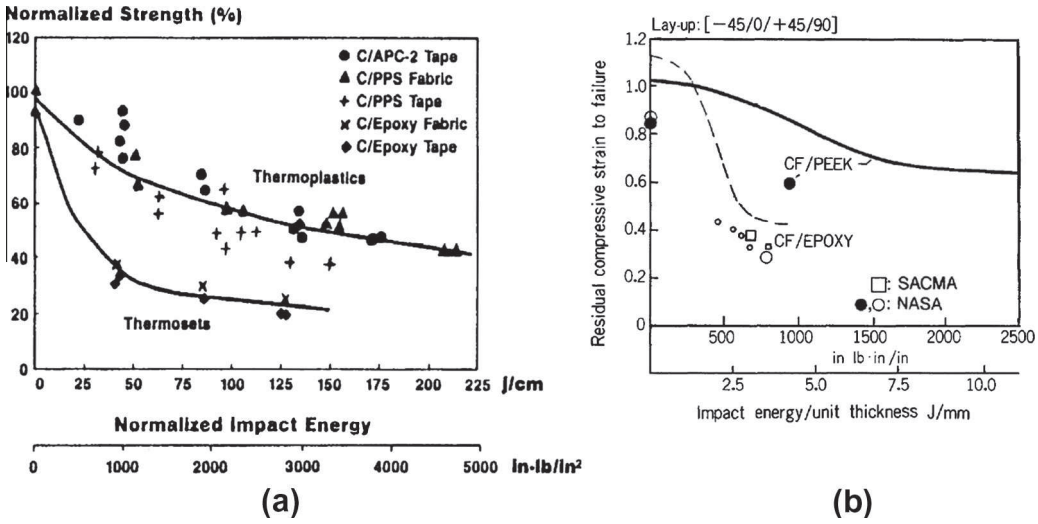

Fig. 1. Comparison of the CAI properties of TP- and TS-based laminates as a function of the impact energy: (a) normalized strength [33] – compressive strain to failure [8].

The process of delamination propagation in the final stage of C/Epoxy CAI tests is well understood: delamination causes buckling deflection reverse in the impact side and reduces the load carrying capacity of the delaminated plates. Due to the ability to arrest delamination, the CAI strain of C/PEEK laminates is almost twice that of C/epoxy (see Fig. 1b), whereas the CAI residual strength is 70% reduced in TS-based laminates and 50% reduced in TP-based laminates at higher impact energy [33].

1.2. About damage tolerance of woven-ply laminates

In addition to the contribution of the matrix toughness to the impact performance of a composite system, the impact behavior and the damage tolerance are also importantly influenced by the reinforcement architecture. The issue of the specific impact behaviors of UD-ply laminates and woven-ply laminates has been well addressed in [10–12,19,20,33–40]. An illustration of the significant contribution of fiber reinforcement to impact behavior is given by Ghasemi Nejhad and Parvizi-Majidi who studied the impact behavior and damage tolerance of carbon-fiber woven-ply TP-based (PEEK and PPS) laminates [20]. The CAI strength of PEEK-based composite remained at 47% of the value for virgin material even after sustaining an impact of 29 J. The features and failure mechanisms are identified [41–42]: inherent toughness of the fabric; the availability of matrix-rich regions at the fiber bundles crimps where plastic deformation can develop along with micro-buckling; crack propagation along the undulating pattern of the yarns creating a large fracture surface area; and multiple crack delaminations on the impacted side [12]. Thus, woven-ply laminates generally exhibit a lower peak load, a smaller damage area, a higher ductility index, and a higher residual CAI strength than UD cross-ply laminates [34], because they show much higher G_{IC} values (often more than 4–5 times) than the UD counter-parts. As a result, the damage tolerance of woven-ply laminates is better, but the overall mechanical properties of non-impacted UD-ply laminates are higher. From this brief literature review, it seemed necessary to look further into matrix's specific contribution (toughness and ductility) to the impact performance, and damage tolerance of different types of woven-ply laminates. To this aim, low velocity impact tests have been conducted at different impact energies [43]. In this work dealing only with the impact behavior, C-scan inspections and a fractography analysis showed that C/TP laminates are characterized by reduced damage (C/PPS laminates in particular), confirming that a tougher matrix can possibly be associated with better impact performance. In addition, the reinforcement weave structure limits extensive growth of delamination, but fiber breakages are more common and appear at lower impact energies because of fiber crimps. The permanent indentation (representative of local matrix crushing or plasticization, and local fiber breakage) can be ascribed to specific mechanisms. In TP-based laminates, the matrix plasticization seems to play an important role in matrix-rich areas by locally promoting permanent deformations. Fiber-bridging also prevents the plies from opening in mode I, and slows down the propagation of interlaminar and intralaminar cracks. Both mechanisms seem to reduce the extension of damages, in particular, the subsequent delamination for a given impact energy. In epoxy-based laminates, the debris of broken fibers and matrix get stuck in the cracks and the adjacent layers, and create a sort of blocking system that prevents the cracks and delamination from closing after impact [44].

1.3. Objectives of the study

In order to assess the severity of damage on the compressive residual strength and behavior, CAI tests were carried out on specimens impacted in [43]. To the authors' knowledge, most of the previous studies focused on the values of residual strength, but do not shed light on a detailed understanding of damage mechanisms leading to the final failure under compressive loading. In general, the compressive residual strength is determined by the

Table 2
Material properties of the different composite systems and buckling theoretical strength of non-impacted specimens [43].

	C/PEEK	C/PPS	C/Epoxy
Ply thickness (mm)	0.32	0.33	0.30
E_{xx} (GPa)	59.1	56.5	63.3
E_{yy} (GPa)	59.4	58.2	63.7
G_{xy} (GPa)	4.04	4.08	5.1
σ_{comp}^{ult} (MPa) $[0]_7$	716	710	731
Stacking sequence	[0/45/0/45/0/45/0]		$[0/45/-45/0]_S$
σ_{comp}^{ult} (MPa)	491	479	513
$\sigma_x^{buckling}$ (MPa)	318	323	330

resistance to buckling of the sub-laminates rather than their in-place resistance [8,14,15]. The buckling of sub-laminates, called "local buckling", is mainly influenced by delamination which depends on the level of impact energy [45,46]. Ply clustering has potential to increase delamination which splits the laminate into sub-laminates, but it results in a lower damage resistance [47]. However, this phenomenon is not sufficient to explain the final failure of the laminates, since in most cases the delamination does not propagate over the entire width of the plate, and the compressive failure is due to the propagation of a crack transversely to the loading direction, from the impact zone to the specimen's edges. In woven-ply laminates, the onset of the final failure is assumed to be induced by local compression failure at the edge of the damage [48,49], but transversal cracks may appear before 80% of the final failure load during CAI tests [50]. These cracks may result from micro-buckling of fibers in the 0° plies. However, the nature and the origin of these cracks (fiber failure in compression, or fiber failure due to buckling) are not discussed in these references.

As a result, the objective of the present work is to further investigate the mechanisms leading to the compressive failure of impact-damaged laminates. From multi-instrumented CAI tests (Digital Image Stereo-Correlation), the role of initial damage (delamination, post-impact cracks, permanent indentation, etc.) on the onset of buckling and cracks development during CAI loadings is analyzed.

2. Experimental setup

2.1. Materials

The composite materials studied in this work are carbon fabric-reinforced prepreg laminated plates consisting of different matrix systems: TP (PPS or PEEK) and TS (Epoxy). The PPS resin (Fortron 0214) is supplied by Ticona, the PEEK resin (grade 150) is supplied by Victrex, and the epoxy resin (914) is supplied by Hexcel. The woven-ply prepreg laminate consists of 5-harness satin weave carbon fiber fabrics whose reference is T300 3K 5HS, and is supplied by SOFICAR. The volume fraction of fibers is 50%. The prepreg plates are hot pressed according to a Quasi-Isotropic lay-up: [(0,90)/(±45)/(0,90)/(±45)/(0,90)/(±45)/(0,90)] in TP-based laminates, and [(0,90)/(±45)/(±45)/(0,90)/(0,90)/(±45)/(±45)/(0,90)] in C/Epoxy. The lay-up slightly differs in order to get similar laminates' thicknesses. The laminates' thickness was averaged from measurements at different points: 2.24 mm in C/PEEK, 2.31 mm in C/PPS, and 2.4 mm in C/Epoxy laminates. The $100 \times 150 mm^2$ specimens were cut from $600 * 600\ mm^2$ flat panels using a

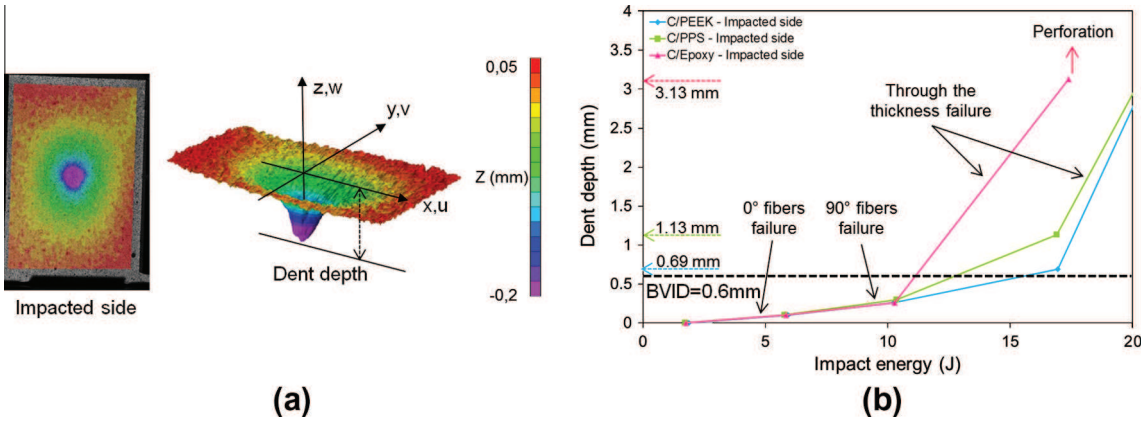

Fig. 2. Dent depth: (a) contour plot and corresponding 3-D image of damaged specimen – (b) Changes in dent depth as a function of the impact energy on the impacted side of specimens.

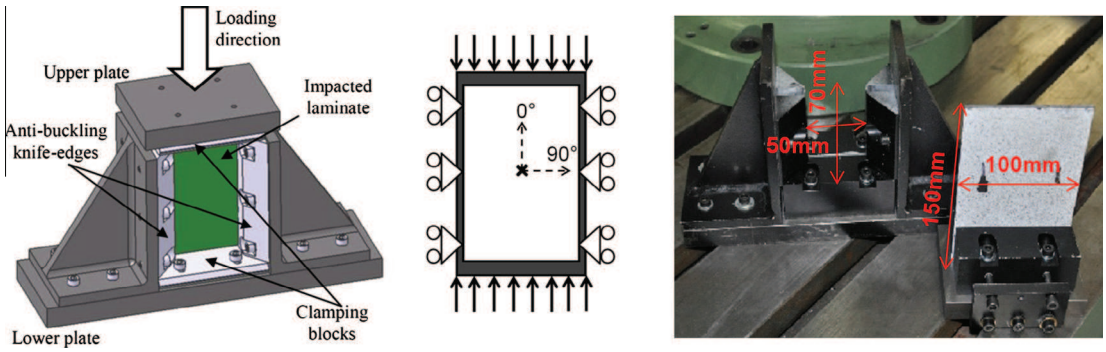

Fig. 3. Compression after impact tests: experimental set-up and anti-buckling fixture.

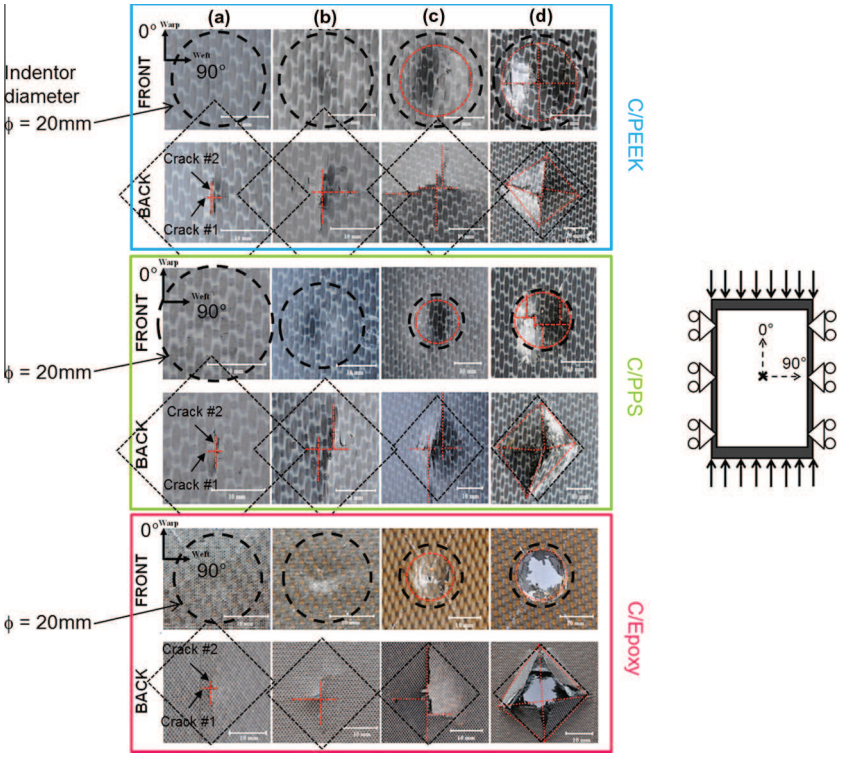

Fig. 4. Observations of impact damage patterns on front and back sides of impacted specimens as a function of the impact energy [43]: (a) 6 J – (b) 10.5 J – (c) 17 J – (d) 25 J.

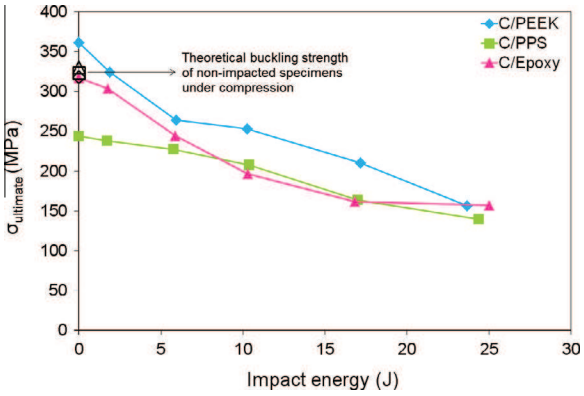

Fig. 5. Ultimate compressive strength as a function of impact energy.

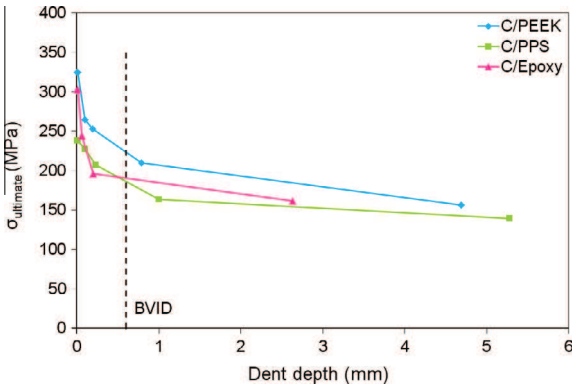

Fig. 6. Ultimate compressive strength as a function of dent depth.

water-cooled diamond saw, and comply with the standard Airbus AITM 1-0010, except for the recommended thickness (4 mm). The main mechanical properties (see Table 2) of the three composite systems investigated in this work have been evaluated in previous works [29,51,52].

2.2. Experimental procedure

2.2.1. Compression-after-impact testing

Low velocity impact tests have been conducted at room temperature on the three composite materials for different impact energies: 2 J, 6 J, 10.5 J, 17 J, 25 J. The experimental set-up is described in [43]. Once the specimens have been impacted, their residual strength is evaluated by means of CAI (Compression after impact) tests, commonly used in the aerospace industry. All the CAI tests were performed using a 100 kN capacity load cell of a Schenk servo-hydraulic testing machine at room moisture (50%). The specimen is placed within a special fixture originally designed by Boeing, which incorporates adjustable side plates to accommodate for both variations in thickness and overall dimension, as well as to prevent specimen buckling (see Fig. 3). Such a compression after impact fixture is placed between the compression platens of the testing machine. The specimens were therefore subjected to compressive loadings at a constant displacement rate $V = 0.2$ mm/min. The objectives of the CAI tests are usually twofold: to evaluate the critical buckling stress and to assess the compressive failure strength. On the front side of the impacted specimen, an extensometer is positioned on a corner of the plate, as far as possible of the expected buckling zone. This extensometer measures the strain in the longitudinal direction ε_x. The out-of plane deflection w_{LVDT} is measured thanks to one LVDT sensor, positioned perpendicularly to the laminates surface and at the center of the specimen, where the largest out-of plane displacement due to compressive loading should be observed. Another LVDT sensor is used to measure the longitudinal displacement $u_{machine}$ of the machine's lower grip.

The experimental set-up monitors four different signals: longitudinal strain ε_x, displacement and force, as well as the out-of plane deflection w.

2.2.2. 3D Digital Image Correlation technique

As impact leads to local damage, a 3D Digital Image Correlation technique can be used to detect singularities of the strain field for impacted plates subjected to compressive loads [53,54]. From CAI tests, it is indeed possible to follow the propagation of impact-induced transversal cracks and the changes in the strain fields (compressive and flexural strains) on both sides of the impacted specimen. Thereby, a video system consisting of two CCD cameras can be used in order to follow the propagation of cracks, and the 3D heterogeneous strains fields can be evaluated during compressive tests. Thanks to the observation of every point from two different vantage points (where the cameras are placed), the device gives the coordinates (x, y, z) of points in a Cartesian coordinate system whose origin is approximately the impact point (see Fig. 2a). Before performing the CAI tests, the spatial arrangement of the cameras is unknown. In order to make the calibration and set up the parameters, a series of pictures of a black and white pattern is taken. As the software is capable of determining the geometry of the pattern, the spatial arrangement of the cameras can be calculated. Once the device is calibrated, the cameras are able to correlate a random pattern. The software used for handling the cameras is supplied by the Society Correlated Solutions. During CAI tests, a pair of digital pictures was taken with Vic-Snap software every 5 kN until laminates failure. On the impacted side of the laminates, the relative displacements (u, v, w) of every point can be measured with respect to its original position, by using the Vic-3D software (see Fig. 2a). The different strains fields $(\varepsilon_x, \varepsilon_y, \varepsilon_z)$ can therefore be obtained from the displacement fields.

3. Results

Impact initiates damages and permanent indentation in laminates, which are instrumental in driving the compressive behavior (and residual strength) of impacted specimens. More particularly, transverse cracks and diamond-shaped fracture patterns (associated with permanent indentation) may lead to premature buckling of specimens. The Barely Visible Damage BVID (0.6 mm) is reached at about 13 J (C/PPS) and 16 J (C/PEEK) in TP-based laminates, whereas it is reached at about 11 J in C/epoxy (see Fig. 2b). Macroscopic views of the front (impacted side) and the back (non-impacted side) of specimens give first information about the onset of damage as a function of the impact energy (see Fig. 4).

The theoretical buckling strength of non-impacted laminates under compression (see Fig. 5) can be classically obtained from the plates theory [55]. The value is virtually the same for the three materials (see Table 2). According to the values of ultimate compressive strengths, the compressive stress in 0° layers at failure is much higher than the theoretical buckling strength. It therefore suggests that buckling occurs very early during the compressive loading of non-impacted specimens. In impacted laminates, the compressive residual strength gradually decreases as impact energy increases (see Fig. 5). At low impact energy (e.g. 2 J), the residual strength of PEEK-based laminates is about 10% and 40% higher than C/Epoxy and C/PPS laminates respectively. At intermediate impact energies, CAI strength of C/PEEK is about 20–30% higher than the one of C/Epoxy and C/PPS. At high impact energy (e.g. 25 J), the residual strength is virtually the same for the three composite systems. Another way to analyze these results is to consider the permanent indentation induced by impact. Such an indentation is ascribed to specific impact damage mechanisms discussed in [43], and is represented by the dent depth which seems to be of the utmost importance from the residual strength standpoint, as it may facilitate local buckling (see Fig. 6). The dent depth is associated with the blistering of the plate [43], from which buckling can be induced. From the results presented in Fig. 6, it appears that the residual strength decreases dramatically for very small values of dent depth (about 0.1 mm at 5 J) and for low impact energies. In addition, the ultimate compressive strengths tend to saturate to reach a minimum value for dent depths higher than the BVID. The observation of the impacted side of specimens reveals the presence of large transversal cracks along the 90° direction (see crack #1 in Fig. 4) which are induced by impact and associated with the failure of 0° fibers. Depending on the impact energy, these cracks may propagate more or less rapidly (depending on matrix

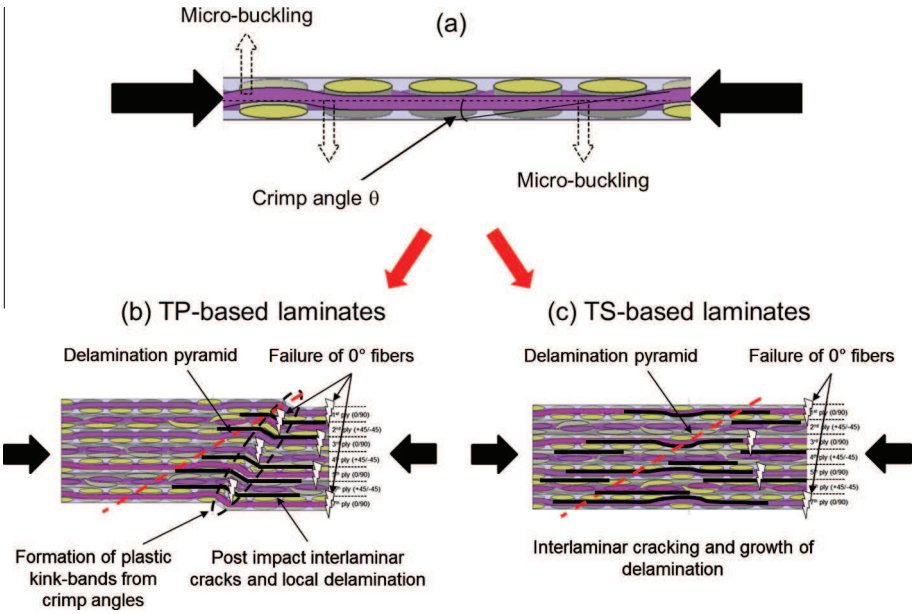

Fig. 7. Mechanisms of compressive failure in woven-ply laminates: (a) micro-buckling of fiber bundles at the crimps in a 5-harness satin weave – (b) formation of plastic kink-bands in TP-based laminates – (c) interlaminar cracking and delamination growth in Epoxy-based laminates.

nature) due to buckling or to compressive loading, ultimately resulting in the failure of specimens. The question is therefore to know which one of the buckling or the compressive loading drives the damage mechanism leading to the propagation of transversal cracks and the subsequent compressive failure of impacted laminates?

4. Discussion

4.1. Compressive response of impact-damaged laminates

The experimental investigations clearly show the presence of two impact-induced cracks along the warp and weft directions

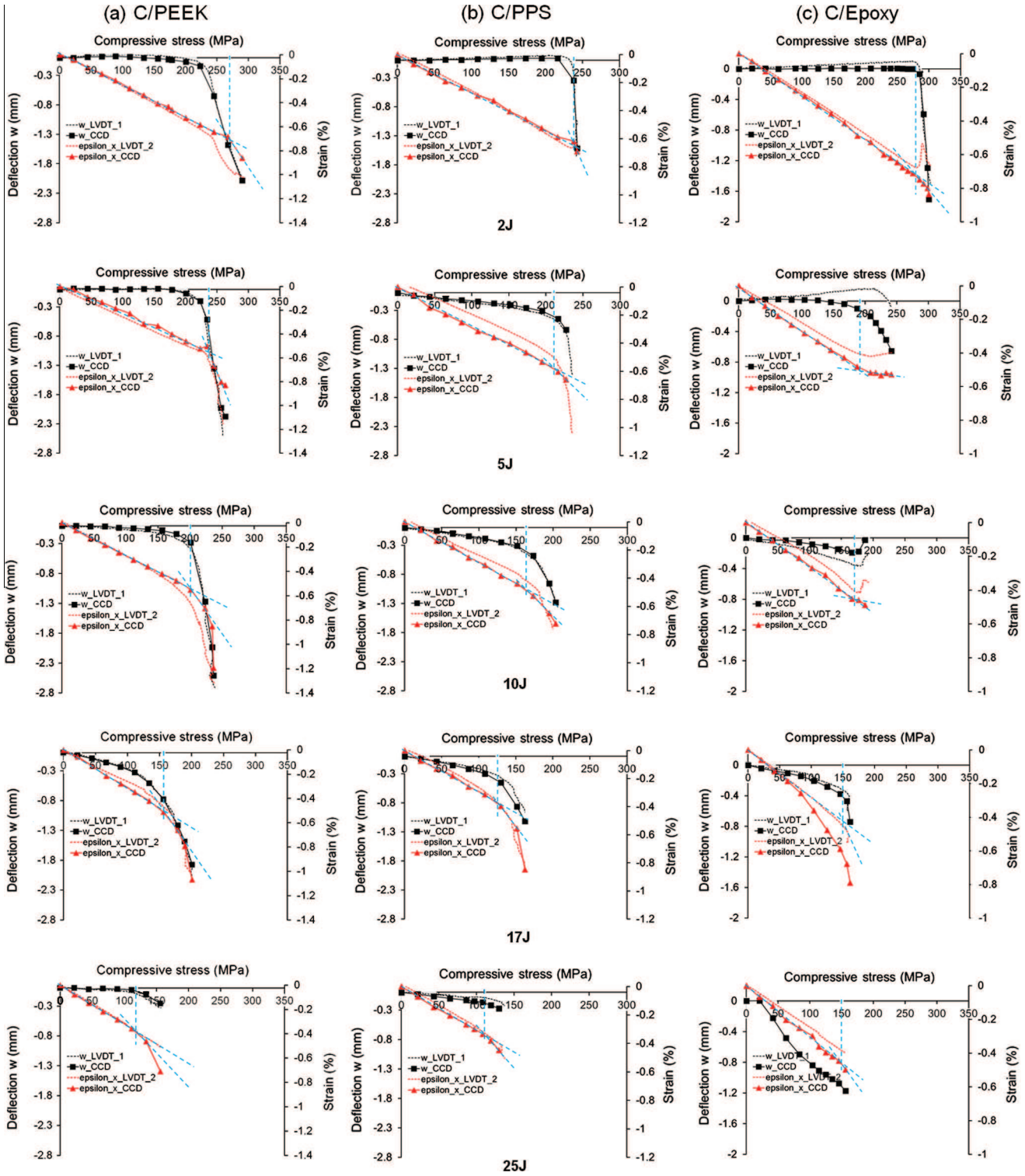

Fig. 8. Transversal deflection and longitudinal strain vs compressive stress during CAI tests on specimens impacted at different impact energies: (a) C/PEEK – (b) C/PPS – (c) C/Epoxy.

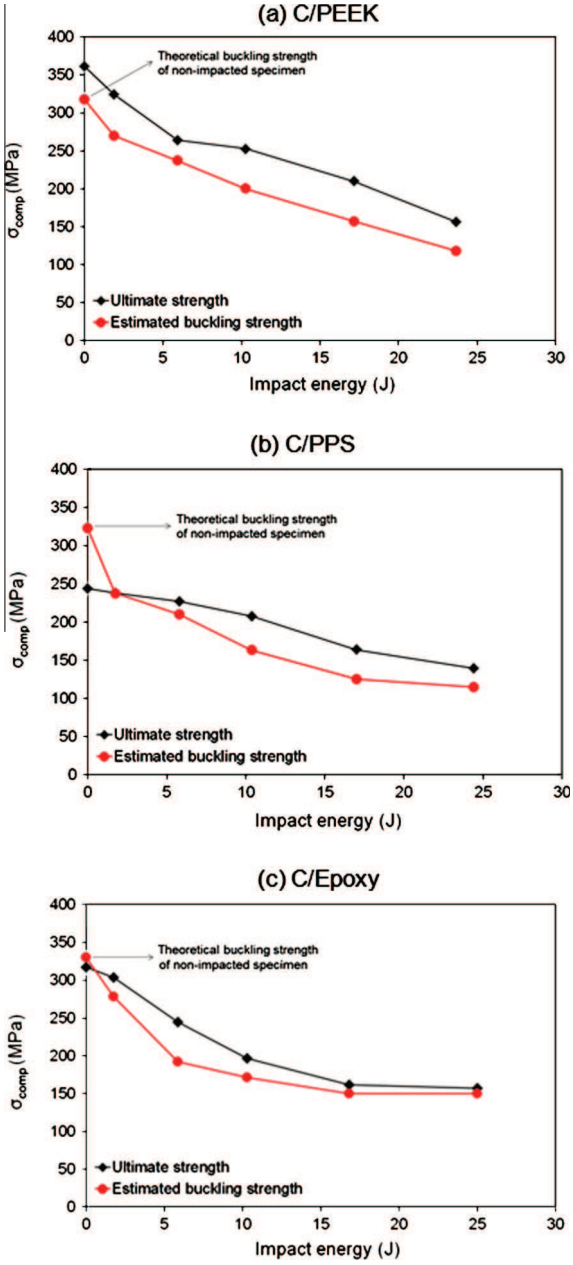

Fig. 9. Comparison of ultimate and experimental critical buckling strength as a function of the impact energy: (a) C/PEEK – (b) C/PPS – (c) C/Epoxy.

on the non-impacted side (see Fig. 4). The CAI tests suggest that the cracks along the 90° direction propagate transversely to the loading direction, whereas the cracks along the 0° direction remains unaltered upon compression in agreement with the conclusions drawn in [54]. At 17 J, the largest delamination under impact loading is observed between the 6th and 7th plies. It is reasonable to consider that the size of the delamination zone between plies increases as a function of thickness as it is represented by the delamination pyramid in [43]. A few prior investigations considered a complete lack of load carrying capacity of the plies within the damaged area [56], resulting in a negligible residual strength in the 5-6-7 plies within the pyramidal damage zone after high impact energy (e.g. 17 J). After low energy impacts (e.g. 2 J), C-scan inspections reveal no visible delamination or cracks [43], hence suggesting that the compressive response of specimens will not be driven by impact-induced damage. Thus, the initial damage

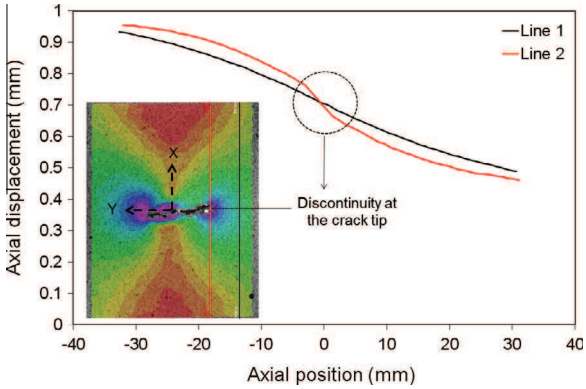

Fig. 10. Method for detecting the tip of transversal cracks associated with 0° fibers failure.

(depending on impact energy) is instrumental in governing the CAI response of laminates.

4.2. Local and micro-buckling

As it is mentioned in Section 1.3, classical global buckling of the plate and local buckling of the delaminated sub-laminates are accompanied by the propagation of transverse cracks on the impacted surface of laminates provided that the impact energy is not too low. Local buckling is facilitated by permanent indentation at high impact energy. Micro-buckling is primary due to the misaligned structure of the weave pattern at the crimps (see Fig. 7a). Both mechanisms are combined during CAI loadings. One of the main purposes of this study is therefore to identify the critical stress at which buckling occurs in impacted laminates. Two different methods can be used:

- The first one consists in evaluating the plate's out-of plane deflection w until the onset of buckling, although most of the specimens actually suffered a reduced increase in their out-of-plane deflection right from the beginning of the tests, because of the impact-induced damage (dent depth). When the critical stress is reached, the deflection suddenly and significantly increases (see Fig. 8). However, it is hard to identify the exact transition point.
- The second method is based on the observation of the longitudinal strain ε_x. Its behavior is linear under pure compression, and the linearity is lost when the plate starts buckling. Normally, this transition point can be more easily determined by observing the changes in the longitudinal strain than in the out-of-plane deflection (see Fig. 8). Thus, it is quite complicated to determine a precise value of this critical stress, and that is the reason why the corresponding value has been estimated from the curves representing longitudinal strain ε_x vs compressive stress.

For each method, the out-of-plane deflection w or the longitudinal strain ε_x can be obtained either from the LVDT sensors or from the CCD cameras (thanks to the 3D Digital Image Correlation). Thus, the second method based on the changes in ε_{xCCD} gives an experimental critical buckling strength (see Fig. 8) which can be compared to the ultimate compressive strength for every impact energy (see Fig. 9). During compressive loading, local buckling appears lately, and the buckling strength significantly decreases as impact-induced damage increases. In TP-based laminates, the buckling strength is about 20% lower than the CAI strength as impact energy increases (see Fig. 9a–b). In TS-based laminates, the

values of both residual compressive strength and buckling strength tend to be the same as impact energy (initial damage) increases (see Fig. 9c). It suggests that the initial damage induced by impact (associated with the specimens' blistering and dent depth) makes local buckling a primary compressive failure mode at high impact energy.

4.3. Propagation of transversal cracks

Once the buckling strength is estimated, it is necessary to evaluate the compressive stress from which the transversal cracks associated with the failure of 0° fibers propagate (see crack #1 in Fig. 4). The initial length of transversal cracks only depends on the impact and permanent indentation. During CAI tests, the propagation of these impact-induced cracks can be locally observed by using the longitudinal displacement field resulting from the DIC analysis. Indeed, the curve representing the axial displacement as a function of the axial position is virtually continuous along line 1 drawn far from the crack (see Fig. 10). The transversal crack tip can be detected when a discontinuity is observed on the curve (see line 2 in Fig. 10), because such discontinuity indicates that the displacement of the upper part is higher than the lower part's one. One digital image being taken every 5 kN during compressive loading, the crack tip can be located from discontinuities appearing on each displacement field. Thus, this method can be used to investigate the propagation of transversal cracks as compressive stress increases for the three materials and every impact energy (see Fig. 11). It is worth noticing that the initial length of these cracks increases as the impact energy increases. For all impacted C/PPS laminates, the length of the crack remains constant (no propagation) until the compressive stress reaches the experimental critical buckling strength where the crack propagates suddenly (see Fig. 11b). It therefore suggests that buckling is instrumental in driving compressive failure in PPS-based composites at any impact energy. On the contrary, slow crack propagation can be observed in PEEK- and Epoxy-based laminates under low compressive stresses (see Fig. 11a and c), suggesting that compressive load governs the compressive failure of 0° fibers of specimens initially subjected to impact energies ranging from 6 to 25 J. The crack propagation becomes therefore accelerates as compressive stress reaches the estimated buckling strength. At low impact energy (e.g. 2 J), cracks propagate suddenly once the compressive stress is higher than the estimated buckling strength, suggesting that buckling drives the compressive failure. A particular attention has been paid to the CAI tests carried out on specimens impacted at 17 J, because such impact energy is higher than the energy level for which the BVID is reached: 16 J in C/PEEK, 13 J in C/PPS, and 11 J in C/Epoxy. As it was indicated in Section 4, a 17 J impact promotes permanent indentation which is closely associated with local buckling. On such specimens, the observations of longitudinal strain fields along with the compressive stress and the crack propagation confirm the previous failure mechanisms: transversal cracks start propagating for compressive stress lower than the estimated buckling strength (at about 111 MPa and 100 MPa, for C/PEEK and C/Epoxy respectively). The propagation is slow until the compressive stress reaches $\sigma_x^{buckling}$ where the propagation becomes rapider as local buckling accelerates the propagation in C/Epoxy (see Fig. 12). The contribution of local buckling to the rapid crack propagation ultimately leads to the failure of these specimens. The main difference between C/Epoxy and C/PEEK is that PEEK matrix intrinsic toughness may counter-balance the effect of local buckling, resulting in relatively slow crack propagation (see Fig. 13). It therefore explains a better damage tolerance as the residual compressive strength is 30% higher in C/PEEK than in C/Epoxy laminates. It is also worth noticing that, comparatively

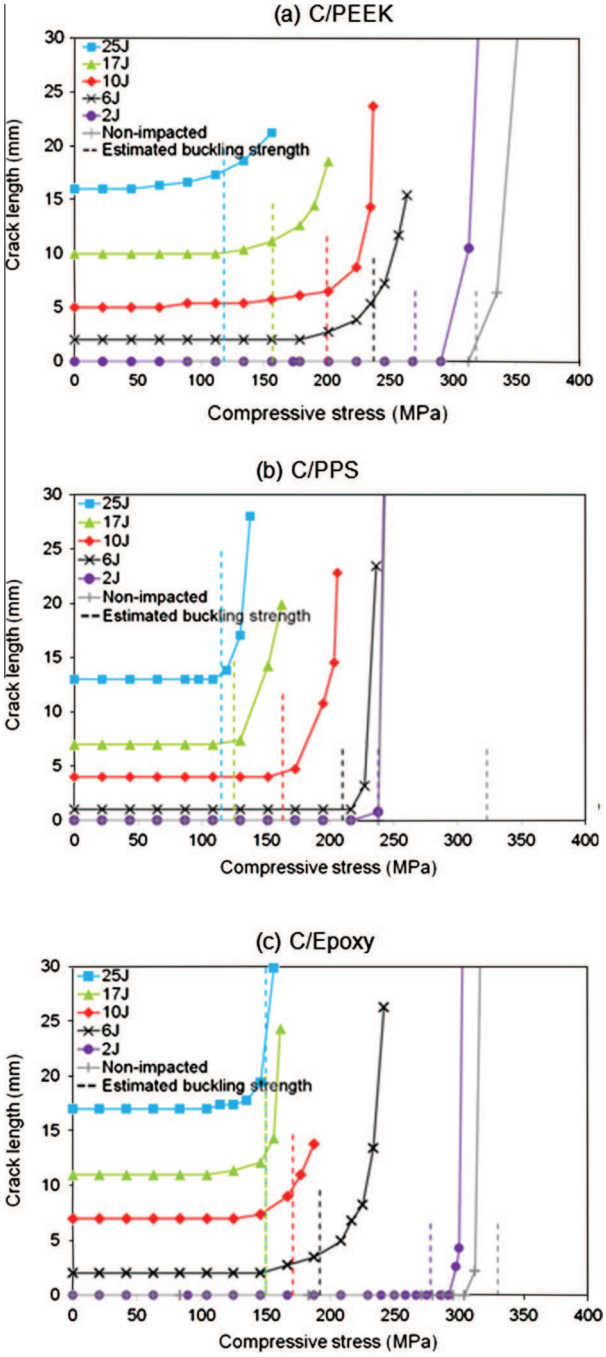

Fig. 11. Propagation of transversal cracks during CAI tests on specimens impacted at different impact energies: (a) C/PEEK – (b) C/PPS – (c) C/Epoxy.

to Epoxy-based laminates, cracks start propagating earlier in C/PEEK during compressive loading, probably due to significantly different initial damage (more extensive delamination and less 0° fibers breakage in C/Epoxy). As 0° fibers breakage is instrumental in driving the CAI behavior, it is reasonable to consider that more impact-induced fiber breakage in C/PEEK laminates results in an earlier propagation. Finally, in C/PPS specimens, the crack length remains virtually unchanged (see Fig. 14), until the compressive stress reaches the estimated buckling strength (at about 125 MPa) where the propagation becomes rapider due to buckling. The highly ductile behavior of PPS matrix may contribute to plastic deformation due to micro-buckling at the crimps, which can delay the cracks onset and subsequent propagation.

4.4. Contribution of matrix ductility and toughness to the CAI failure

From CAI tests combined with Digital Image Stereo-Correlation, the role of initial damage (delamination, post-impact cracks, permanent indentation, etc.) on the onset of buckling and cracks development during CAI loadings has been investigated. It allowed the authors to establish a damage scenario resulting in the ultimate failure of impacted laminates provided that the impact energy is not too low: (i) The plate first responds linearly to in-plane plane compression – (ii) Buckling appears in a combination of global buckling of the plate, and local buckling at the center of the plate – (iii) The curvature due to global buckling increases compressive stresses at the tips of transversal cracks, leading the cracks to propagate more or less rapidly depending on the matrix toughness and ductility – (iv) The crack propagation accelerates and leads to the ultimate failure of specimens.

However, it appears that the previous scenario may differ from one material to another, depending on the contribution of matrix ductility [52] and toughness (see Table 1) to the CAI failure of the studied woven-ply laminates. The compressive failure is usually governed by three primary mechanisms in composite laminates [57]: (i) Buckle delamination is associated with low toughness matrix (typically in Epoxy-based laminates), and the presence of local delamination – (ii) Out-of-plane shearing leading to the fragmentation of the plies and local buckling of 0° fiber bundles. Such a mechanism is mostly based on the breakage of 0° fibers – (iii) Splaying of external plies. Such a mechanism is associated with a longitudinal splitting between 0° fibers bundles in low ductility matrix (typically in Epoxy-based laminates).

During CAI tests, other compressive failure modes are possible, and usually result from a combination of the previous mechanisms. It is also known that carbon fibers under compressive loadings are prone to global instabilities [58], and the initial alignment of fibers in reinforced composites has a large influence on their compressive response [59]. Thus, the crimp region plays a significant role in controlling the onset of failure in woven-ply

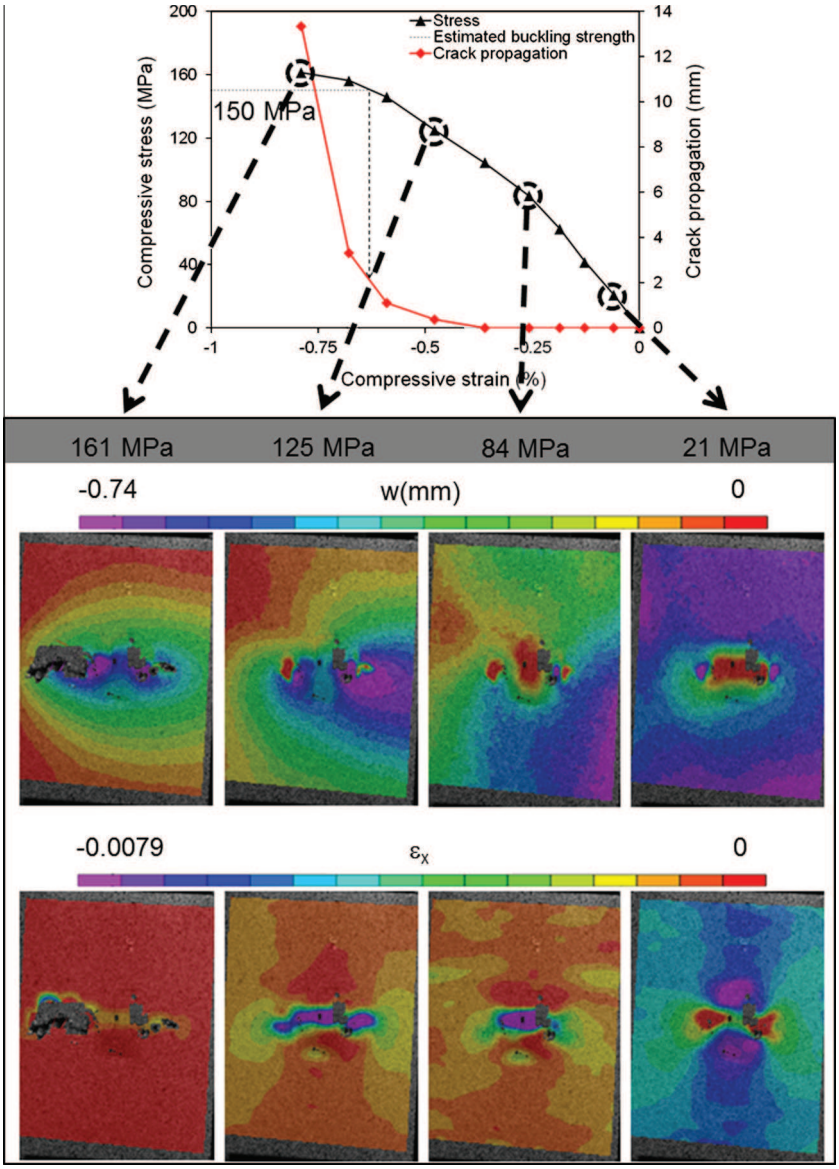

Fig. 12. CAI response of C/Epoxy laminates after a 17 J impact: correspondence of the crack propagation with transversal displacement w and longitudinal strain ε_x fields at different compressive stresses.

laminates, mostly because of the undulating structure of carbon fabrics (see Fig. 7a), and the presence of matrix-rich areas at the crimps [56,60,61]. Both matrix toughness and ductility contribute to specific failure mechanisms within a fiber network. In woven-ply misaligned structures, micro-buckling at the crimps is found to cause fiber crushing and the possible onset of highly deformed inclined kink-band formation. In Epoxy-based specimens, the micro-buckling is combined with local buckling of the sub-laminates resulting from permanent indentation. Micro-buckling leads to the interlaminar cracking at the crimps, whereas local buckling promotes the growth of delamination, and ultimately the failure of 0° fibers in the [(0,90)] plies of the laminates (see Fig. 7c). In TP-based laminates, local and micro-buckling also operate even though the effect of local buckling is more significant in C/PEEK than in C/PPS because the dent depth is higher. In addition, micro-buckling comes along with a plastic deformation of the matrix in highly ductile matrix systems (such as PPS-based laminates), resulting in the formation of plastic kink-bands, also called plastic buckling (see Fig. 7b) [60,62]. Such plastic buckling may delay the onset and subsequent propagation of transversal cracks during compressive loadings, whereas the local buckling of the delaminated sub-laminates is instrumental in accelerating the propagation of transverse cracks (failure of 0° fibers) in the [(0,90)] plies of the laminates. PEEK-based composite have a less ductile behavior than the one observed in C/PPS [50], ultimately leading to the formation of less plastic kink-bands. In addition and as far the mode II interlaminar fracture is concerned (see Table 1), C/PEEK laminates are about 3 times tougher than C/PPS and C/Epoxy [43]. The CAI results suggest that the matrix toughness of TP-based resins (particularly C/PEEK) is not completely transferred to the reinforced polymer. As indicated in Section 4.3, the matrix toughness should counter-balance the effect of local buckling. However, the significant permanent indentation facilitates local buckling, which becomes a primary compressive failure mode at high impact energy. It could therefore justify why the much higher toughness of TP-based laminates (particularly C/PEEK) does not result in significantly higher CAI residual strengths in relation to the one obtained in C/Epoxy laminates.

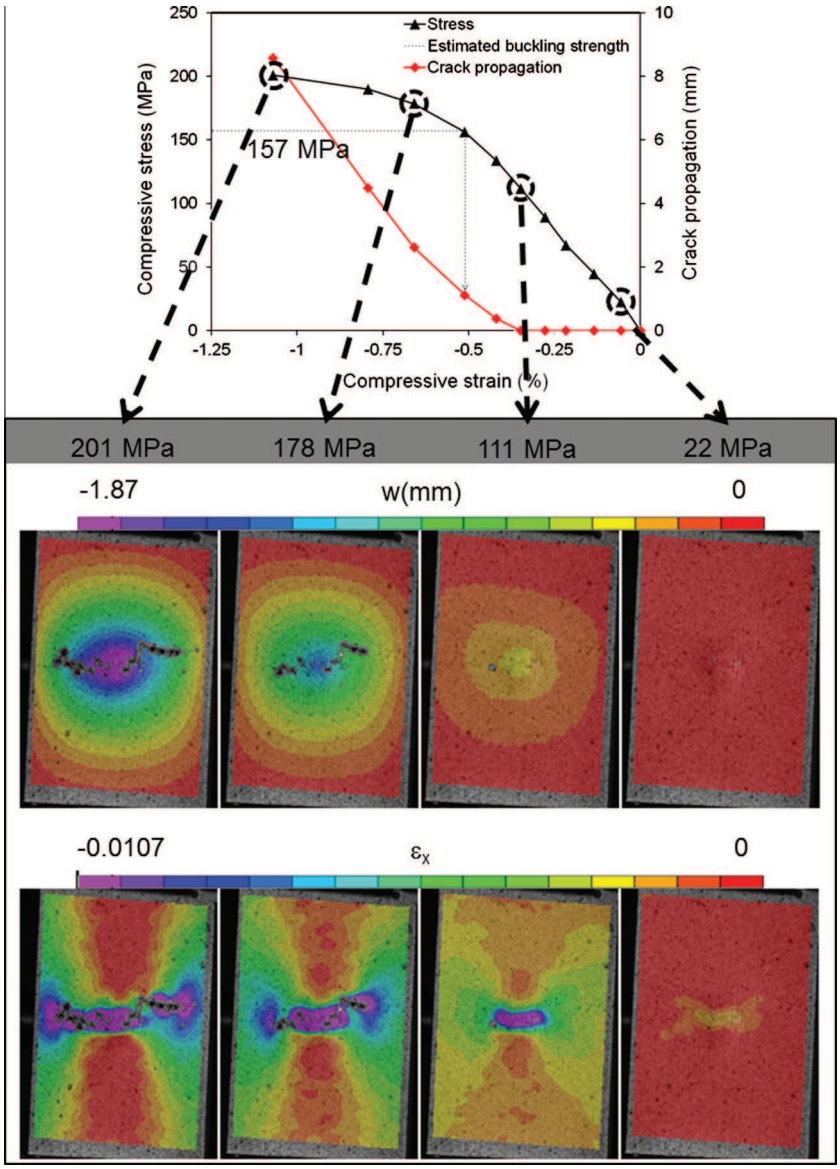

Fig. 13. CAI response of C/PEEK laminates after a 17 J impact: correspondence of the crack propagation with transversal displacement w and longitudinal strain ε_x fields at different compressive stresses.

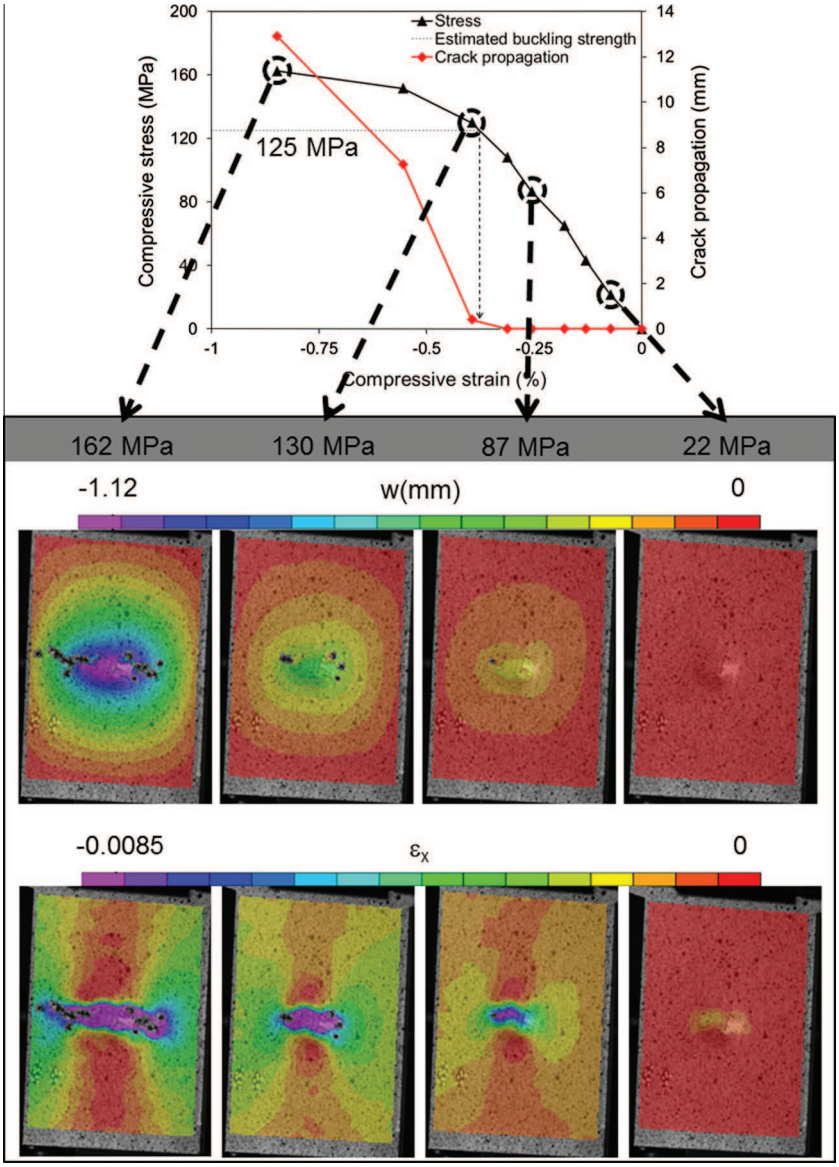

Fig. 14. CAI response of C/PPS laminates after a 17 J impact: correspondence of the crack propagation with transversal displacement w and longitudinal strain ε_x fields at different compressive stresses.

5. Conclusion

The present work was aimed at investigating the mechanisms leading to the compressive failure of impact-damaged laminates consisting of a more or less tough and ductile matrix. From CAI tests combined with Digital Image Stereo-Correlation, the role of initial damage (delamination, post-impact cracks, permanent indentation, etc.) on the onset of buckling and transversal cracks (failure of 0° fiber bundles) development during CAI loadings is analyzed. At low impact energy, the CAI residual strength of PEEK-based laminates is about 10% and 40% higher than C/Epoxy and C/PPS laminates respectively, whereas it is virtually the same for the three composite systems at high impact energy.

During CAI loadings, local buckling is a primary compressive failure mode particularly at high impact energy. Buckling appears in a combination of local buckling of sub-laminates resulting from permanent indentation, and a micro-buckling at the crimps. Provided that the impact energy is not too low, the permanent indentation is associated with the blistering of the plate after impact, which seems to be of the utmost importance from the residual strength standpoint, as it may facilitate local buckling. Micro-buckling seems to be primarily ascribed to the misaligned structure of the weave pattern at the crimps.

In Epoxy-based laminates, micro-buckling leads to the inter-laminar cracking at the crimps, whereas local buckling promotes the growth of delamination, and ultimately the failure of 0° fibers in the [(0,90)] plies of the laminates. In TP-based laminates, micro-buckling comes along with a plastic deformation of the matrix in highly ductile matrix systems (such as PPS-based laminates), resulting in plastic buckling. Such plastic buckling may delay the onset and subsequent propagation of transversal cracks during compressive loadings, whereas local buckling is instrumental in accelerating the propagation of transverse cracks in the [(0,90)] plies of the laminates. The matrix toughness should counter-balance the effect of local buckling. However, the latter effect becomes a primary compressive failure mode at high impact energy, as it is facilitated by a significant permanent indentation. It could therefore justify why the much higher toughness of TP-based laminates

(particularly C/PEEK) does not result in significantly higher CAI residual strengths in relation to the one obtained in C/Epoxy laminates.

References

[1] Cantwell WJ, Morton J. The impact resistance of composite materials – a review. Composites 1991;22(5):347–62.
[2] Jang BP, Kowbel W, Jang BZ. Impact behavior and impact-fatigue testing of polymer composites. Compos Sci Technol 1992;44(2):107–18.
[3] Abrate S. Impact on composites structures. Cambridge University Press; 1998.
[4] Hancox NL. An overview of the impact behavior of fibre-reinforced composites. In: Reid SR, Zhou G, editors. Impact behavior of fiber-reinforced composite materials and structures. CRC Press, Woodhead Pub. Ltd.; 2000.
[5] Bibo GA, Leicy D, Hogg PJ, Kemp M. High-temperature damage tolerance of CRFP: Part 1: impact characteristics. Composites 1994;25(6):414–24.
[6] Bibo GA, Hogg PJ, Kemp M. High-temperature damage tolerance of CRFP: 2. Post-impact compression characteristics. Composites 1995;26(2):91–102.
[7] Jang BP, Huang CT, Hsieh CY, Kowbel W, Jang BZ. Repeated impact failure of continuous fiber reinforced thermoplastic and thermoset composites. J Compos Mater 1991;25(9):1171–203.
[8] Ishikawa T, Sugimoto S, Matsushima M, Hayashi Y. Some experimental findings in CAI tests of CF/PEEK and conventional CF/Epoxy flat plates. Compos Sci Technol 1995;55:349–63.
[9] Davies P, Riou L, Mazeas F, Warnier P. Thermoplastic composite cylinders for underwater applications. J Thermop Compos Mater 2005;18(5):417–43.
[10] Schrauwen B, Peijs T. Influence of matrix ductility and fibre architecture on the repeated impact response of glass-fibre-reinforced laminated composites. Appl Compos Mater 2002;9(6):331–52.
[11] Kim J-K, Sham M-L. Impact and delamination failure of woven-fabric composites. Compos Sci Technol 2000;60:745–61.
[12] Bibo GA, Hogg PJ. Review: the role of reinforcement architecture in impact damage mechanisms and post-impact compression behavior. J Mater Sci 1996;31:1115–37.
[13] Mili F, Necib B. Impact behavior of cross-ply laminated composite plates under low velocities. Compos Struct 2001;51(3):237–44.
[14] Aktaş M, Atas C, İçten BM, Karakuzu R. An experimental investigation of the impact response of composite laminates. Compos Struct 2009;87(4):307–13.
[15] Reis PNB, Ferreira JAM, Santos P, Richardson MOW, Santos JB. Impact response of Kevlar composites with filled epoxy matrix. Compos Struct 2012;94(12):3520–8.
[16] Morton J, Godwin EW. Impact response of tough carbon fibre composites. Compos Struct 1989;13(1):1–19.
[17] Prevorsek DC, Chin HB, Bhatnagar A. Damage tolerance: design for structural integrity and penetration. Compos Struct 1993;23(2):137–48.
[18] Bartus SD, Vaidya UK. Performance of long fiber reinforced thermoplastics subjected to transverse intermediate velocity blunt object impact. Compos Struct 2005;67(3):263–77.
[19] Reyes G, Sharma U. Modeling and damage repair of woven thermoplastic composites subjected to low velocity impact. Compos Struct 2010;92(2):523–31.
[20] Ghasemi Nejhad MN, Parvizi-Majidi A. Impact behaviour and damage tolerance of woven carbon fibre-reinforced TP composites. Composites 1990;21(2):155–68.
[21] Wang H, Vu-Khanh T. Damage extension in carbon fiber/PEEK cross ply laminates under low velocity impact. J Compos Mater 1994;28(8):684–707.
[22] Gao S-L, Kim J-K. Cooling rate influence in carbon fibre/PEEK composites. Part III: impact damage performance. Composites Part A 2001;32(6):775–85.
[23] Aymerich F, Priolo P, Vacca D. Static loading and low-velocity impact characterization of graphite/PEEK Laminates. In: Proceedings of the Int Conf on Adv Mat. Hurghada, Egypt; 1998.
[24] Chaudhuri J, Ghoe GH, Vinson JR. Impact characterization of graphite fiber reinforced thermoplastic laminates. J Reinf Plastics Compos 1993;12(6):67–685.
[25] Vedula M, Koczak MJ. Impact resistance of cross-plied polyphenylene sulfide composites. J Thermop Compos Mater 1989;2(3):154–63.
[26] Spamer GT, Brink NO. Investigation of the CAI properties of C/PPS and C/APC-2 TP materials. In: Proceedings of the 33rd Int SAMPE Symposium: Materials-Pathway to the, Future, 1988.
[27] Ma C-CM, Lee C-L, Chang M-J, Tai N-H. Effect of physical aging on the toughness of CFR PEEK and PPS composites. Polym Compos 1992;13(6):441–7.
[28] Davies GAO. Design methodology to improve damage tolerance in composites. In: 2nd ed., Brite Euram 3159-89 Contract Report, Dept. of Aeronautics, Imperial College, London; 1993.
[29] De Baere I, Jacques S, Van Paepegem W, Degrieck J. Study of the Mode I and Mode II interlaminar behavior of a carbon fabric reinforced TP. Polym Test 2012;31(2):322–32.
[30] Davies P, Benzeggagh ML, De Charentenay FX. The delamination behavior of carbon fiber reinforced PPS. In: 32nd Int SAMPE Symposium, 1987. p. 134–146.
[31] Lachaud F, Lorrain B, Michel L, Barriol R. Experimental and numerical study of delamination caused by local buckling of TP and TS composites. Compos Sci Technol 1997;58:727–33.
[32] O'Brien K. Composite Interlaminar Shear Fracture Toughness GIIc: shear measurement or sheer myth? Tech Memorandum, NASA, 1997.
[33] Spamer GT, Brink NO. In: Proceedings of the 33rd International SAMPE Symposium, 1988. p. 284–295.;
Alif N, Carlsson LA, Boogh L. The effect of weave pattern and crack propagation direction on mode I delamination resistance of woven carbon composites. Composites Part B 1998;29:603–11.
[34] Kim J-K, Leung LM, Lee SWR, Hirai Y. Impact performance of a woven fabric CFRP laminate. Polym Compos 1996;4:549–61.
[35] Funk JG, Deaton JW. The interlaminar fracture toughness of woven graphite/epoxy composites. NASA Tech Paper 2950, 1989.
[36] Siow YP, Shim VPW. An experimental study of low velocity impact damage in woven fiber composites. J Compos Mater 1998;32(12):1178–202.
[37] Jegley DC. Compression behavior of graphite-thermoplastic and graphite-epoxy panels with circular holes or impact damage. NASA Tech Paper, 3071, 1991.
[38] Baker DJ. Mechanical property characterization and impact resistance of selected graphite/PEEK composite materials. NASA Tech Memorandum 102769, AVSCOM Tech, Report 90-B-012, 1991.
[39] Atas C, Sayman O. An overall view on impact response of woven fabric composite plates. Compos Struct 2008;82(3):336–45.
[40] Hongkarnjanakul N, Bouvet C, Rivallant S. Validation of low velocity impact modelling on different stacking sequences of CFRP laminates and influence of fibre failure. Compos Struct 2013;106:549–59.
[41] Karaoğlan L, Noor AK, Kim YH. Frictional contact/impact response of textile composite structures. Compos Struct 1997;37(2):269–80.
[42] Akkerman R, Warnet LL, Van de Ven EC. Impact damage in woven fabric reinforced composites. In: Proceedings of the 10th Int Conf on Textile Comp TEXCOMP'10, Lille, France, October, 2010.
[43] Vieille B, Casado VM, Bouvet C. About the impact behavior of woven-ply carbon fiber-reinforced thermoplastic- and thermosetting-composites: a comparative study. Compos Struct 2013;101:9–21.
[44] Hongkarnjanakul N, Rivallant S, Bouvet C, Miranda A. Permanent indentation characterization for low-velocity impact modelling using three-point bending test. J Compos Mater 2013. http://dx.doi.org/10.1177/0021998313499197.
[45] De Freitas M, Reis L. Failure mechanisms on composite specimens subjected to compression after impact. Compos Struct 1998;42(4):365–73.
[46] Sanchez-Saez S, Barbero E, Zaera R, Navarro C. Compression after impact of thin composite laminates. Compos Sci Technol 2005;65(13):1911–9.
[47] González EV, Maimí P, Camanho PP, Lopes CS, Blanco N. Effects of ply clustering in laminated composite plates under low-velocity impact loading. Compos Sci Technol 2011;71(6):805–17.
[48] Yan H, Oskay C, Krishnan A, Xu LR. Compression-after-impact response of woven fiber-reinforced composites. Compos Sci Technol 2010;70(14):2128–36.
[49] Aktas M, Karakuzu R, Arman Y. Compression-after impact behavior of laminated composite plates subjected to low velocity impact in high temperatures. Compos Struct 2009;89:77–82.
[50] Kinsey A, Saunders DEJ, Soutis C. Post-impact compressive behaviour of low temperature curing woven CFRP laminates. Composites 1995;26:661–7.
[51] Aucher J, Vieille B, Taleb L. Influence de la température sur le comportement mécanique de stratifiés tissés thermoplastique ou thermodurcissable. Rev Comp Mat Av 2011;21(3):317–43.
[52] Vieille B, Aucher J, Taleb L. Woven ply thermoplastic laminates under severe conditions: notched laminates and bolted joints. Composites Part B 2011;42(3):341–9.
[53] Kim JH, Pierron F, Wisnom MR, Avril S. Local stiffness reduction in impacted composite plates from full-field measurement. Composites Part A 2009;40(12):1961–74.
[54] Yu Z, Bataxi, Wang H. Full field strain characteristics of composite laminate with impact damage under in-plane load. In: Proceedings of the 19th International Conference On Composite Materials ICCM19, Montréal, Canada, August, 2013.
[55] Xiang Y, Liew KM, Kitipornchai S. Exact buckling solutions for composite laminates: propers free edge conditions under in-plane loading. Acta Mech 1996;117:115–28.
[56] Naik NK, Joglekar MN, Arya H, Borade SV, Ramakrishna KN. Impact and compression after impact characteristics of plain weave fabric composites: effect of plate thickness. Adv Compos Mater 2004;12:261–80.
[57] Fleck NA. Compressive failure of fiber composites. Adv Appl Mech 1997;33:43–119.
[58] Soutis C, Curtis PT, Fleck NA. Compressive failure of notched carbon fiber composites. Proc Royal Soc A 1909;1993(440):241–56.
[59] Avery DP, Samborsky DD, Mandell JF, Cairns DS. Compression strength of carbon fiber laminates containing flaws with fiber waviness. In: Proceedings of the 42nd AIAA Aerospace Sciences Meeting and Exhibit (2004), pp. 54–63.
[60] Grape JA, Gupta V. The effect of temperature on the strength and failure mechanisms of a woven carbon/polyimide laminate under compression. Mech Mater 1998;30(3):165–80.
[61] Osada T, Nakai A, Hamada H. Initial fracture behavior of satin woven fabric composites. Compos Struct 2003;61(4):333–9.
[62] Pinho ST, Robinson P, Iannucci L. Fracture toughness of the tensile and compressive fibre failure modes in laminated composites. Compos Sci Technol 2006;66(13):2069–79.